Ornamental Plant Research

ARTICLE

Open Access

https://doi.org/10.48130/opr-0024-0028
*Ornamental Plant Research* **2024**, 4: e029

# Alternative splicing of activator *CcbHLH1* gene accounts for anthocyanin absence in white cornflower

Chengyan Deng[1*], Xiaofan Zheng[1], Jiaying Wang[2], Yanfei Li[2], Jingjing Li[2], Min Lu[2], Ruina Gao[1], Chenyuan Ji[1], Qinghe Hao[1] and Silan Dai[2*]

[1] *College of Agriculture and Forestry Science, Linyi University, Linyi 276000, China*
[2] *College of Landscape Architecture, Beijing Forestry University, Beijing 100083, China*
* Corresponding authors, E-mail: dcinya@sina.com; silandai@sina.com

## Abstract

Anthocyanins play crucial roles in conferring multicolored characteristics to higher plant organs. Previous studies have investigated the absence of anthocyanin accumulation in white cornflower petals, where the anthocyanin biosynthesis pathway was obstructed by *CcF3H*. However, the genetic regulation mechanism underlying anthocyanin absence remained unclear. In the present study, the full-length sequences of two transcription activators *CcMYB6-1* and *CcbHLH1* were isolated in white cornflower petals. The multi-sequence alignment analysis revealed that there was no difference in the *CcMYB6-1* sequence between the blue and white petals, while *CcbHLH1* was truncated to a length of 1,125 bp on account of alternative splicing, resulting in a frame-shift mutation and premature codon, leading to the loss of basic, helix-loop-helix domains. The truncated CcbHLH1 could still interact with CcMYB6-1 as demonstrated by yeast-two hybrid and bimolecular luminescence complementary assays but lost the ability to enhance the trans-activation of *CcDFR* promoter using dual-luciferase assay. Transient over-expression of mutated *CcbHLH1* in tobacco leaves resulted in a significant decrease in anthocyanin production. These results suggested the alternative splicing of *CcbHLH1* caused the incapacity of trans-activating the anthocyanin biosynthetic pathway together with *CcMYB6-1*, finally leading to anthocyanin absence in white cornflower. The present findings further shed light on the genetic regulation mechanism of anthocyanin biosynthesis in cornflower and enrich the knowledge underlying the white color transition in higher plants.

**Citation:** Deng C, Zheng X, Wang J, Li Y, Li J, et al. 2024. Alternative splicing of activator *CcbHLH1* gene accounts for anthocyanin absence in white cornflower. *Ornamental Plant Research* 4: e029 https://doi.org/10.48130/opr-0024-0028

## Introduction

Flower color is one of the most important components in floral traits that help higher plants attract pollinators for successful fertilization. There are abundant flower color variations among species, cultivars, and hybrid progenies, in which the white flowers, commonly as a symbol of purity and holiness, play important roles in ceremonial events and ikebana. It is well known that anthocyanins are the core pigments to generate different degrees of red, violet, or blue flowers[1,2]. Comparatively, there were only some colourless co-pigments like flavanones, flavones and flavonols found in the white flowers, such as that seen in the white petals of cornflower, *Scutellaria baicalensis*, and *Cymbidium ensifolium*[3–5]. Namely, anthocyanin absence leads to the white color formation in most higher plants.

Anthocyanin, a subclass of flavonoids, is an important secondary metabolite catalyzed by a series of enzymes[6,7]. Initially, chalcone synthase (CHS) catalyzes the tetrahydroxychalcone synthesis from 4-coumaroyl CoA and malonyl CoA, which was rapidly isomerized to the naringenin by chalcone isomerase (CHI). Then flavanone 3-hydroxylase (F3H) catalyzes the hydroxylation at its 3-position to generate dihydrokaempferol (DHK), which can be further catalyzed by the flavonoid 3'-hydroxylase (F3'H) and flavonoid 3'5'-hydroxylase (F3'5'H) to yield dihydroquercetin (DHQ) and dihydromyricetin (DHM), respectively. DHK, DHQ, and DHM are further converted to pelargonidin, cyanidin, and delphinidin by dihydroflavonol 4-reductase (DFR) and anthocyanidin synthase (ANS), respectively. Finally, sugar molecules and acyl groups are attached to the anthocyanidins by both glycosyltransferase (GT) and acyltransferase (AT). Therefore, any block in the structural genes will trigger anthocyanin deficiency. For example, down-regulation of the early biosynthetic genes, such as *CHS* and *F3H*, led to the white flower phenotypes in *Ipomoea purpurea*, *Torenia fournieri*, *Dahlia variabilis*, gentian, and *C. kanran*[8–13]. Moreover, deficiency of the late biosynthetic genes (*DFR*, *ANS* and *GT*, etc.) also blocked anthocyanin accumulation and facilitated white flower formation, such as the cases in *Salvia miltiorrhiza*, *Aquilegia vulgaris*, strawberry, and *Iris bulleyana*[14–17].

Anthocyanin biosynthetic genes are under the control of a regulatory complex composed of MYB, bHLH, and WD40[18,19]. MYB transcription factors play crucial roles in this process. The mutation of R2R3 MYB transcription activators resulted in the evolutionary transitions to white flowers in *Antirrhinum* and *Petunia*[20,21], while R3 MYBs usually function as transcription inhibitors involved in down-regulating multiple anthocyanin biosynthetic genes, leading to anthocyanin absence in higher plant organs[22–25]. In addition, bHLHs of the IIIf subgroup are involved in anthocyanin biosynthesis, which are further divided into two distinct clades, namely bHLH1 and bHLH2 genes[26]. Usually, the bHLH2 plays essential roles in anthocyanin biosynthesis, and its mutation often results in anthocyanin decrease

© The Author(s)

and color fading[27–30]. Moreover, the bHLH1 proteins in *Arabidopsis thaliana* and *Antirrhinum majus* also directly regulate anthocyanin biosynthesis[31–33].

Our previous study revealed that the transcripts of structural genes involved in anthocyanin biosynthesis, e.g., *CcF3H*, *CcF3'H*, and *CcDFR* were nearly undetectable in the white cornflower petals lacking anthocyanin accumulation[3], which was possibly caused by the upstream transcription factors (TFs). Besides, two TFs, *CcMYB6-1*, and *CcbHLH1*, were identified as activators synergistically regulating anthocyanin biosynthesis in cornflower[34]. In the present study, the anthocyanin accumulation in both vegetative and reproductive organs in two cornflower cultivars were first monitored and it clarified that anthocyanins were completely absent in the white cornflower. To further explore the molecular mechanism underlying the white color transition in cornflower, the transcript abundances of both structural genes and transcription factors involved in anthocyanin biosynthesis were detected, and the full-length sequence of *CcMYB6-1* and *CcbHLH1* were isolated, followed by the multi-sequence alignment and phylogenetic analysis. Subsequently, the genomic sequence of *CcbHLH1* was isolated to elucidate its truncation reason. Furthermore, the subcellular localization analysis, yeast-two hybrid, bimolecular luminescence complementary assay, dual-luciferase assay, as well as the transient over-expression in tobacco leaves were conducted to explore the functional changes after *CcbHLH1* truncation. The findings will enhance our understanding of the regulation mechanism of anthocyanin biosynthesis in cornflower, and provide new insights on the white color transition in higher plants.

## Materials and methods

### Plant material

Two *Centaurea cyanus* cultivars with blue and white petals were used in this study, namely, 'Dwarf Tom Pouce Blue' (DTPB) and 'Dwarf Tom Pouce White' (DTPW) (Fig. 1a). The seeds were purchased from the Outsidepride Seed Source, LLC. Their seeds were sown in an equal volume mixture of peat and vermiculite, then placed in phytotron under 23 °C and 16 h/8 h (light/dark) conditions. After one month of cultivation, the seedlings began to blossom, and capitula were divided into four developmental stages based on our previous publication[3] (Fig. 1b). Briefly, the buds in stage one (S1), stage two (S2), and stage three (S3) were uncolored, less than 50% pigmented, and fully pigmented, respectively, while the petals in stage four (S4) were opened and fully pigmented (Fig. 1c). The roots, stems, leaves, sepals, and petals (S1–S4) were collected into 2 mL RNAase-free tubes, rapidly precooled in liquid nitrogen and stored at −80 °C before use.

### Gene isolation and qRT-PCR analysis

Total RNAs were extracted from petals of DTPW and DTPB, respectively, followed by the first-strand cDNA generation using M-MLV reverse transcriptase (Promega, Germany). Polymerase chain reaction was conducted to amplify the full or partial-length of *CcMYB6-1* and *CcbHLH1* in the two cornflower cultivars. The 3′-rapid amplification of cDNA ends (3'-RACE) was performed to isolate the *CcbHLH1#* in DTPW, followed by verification of the obtained sequence using the high-fidelity enzyme of KOD-201 (TOYOBO, Japan). To further explore the expression characteristics of structural and regulatory genes, the

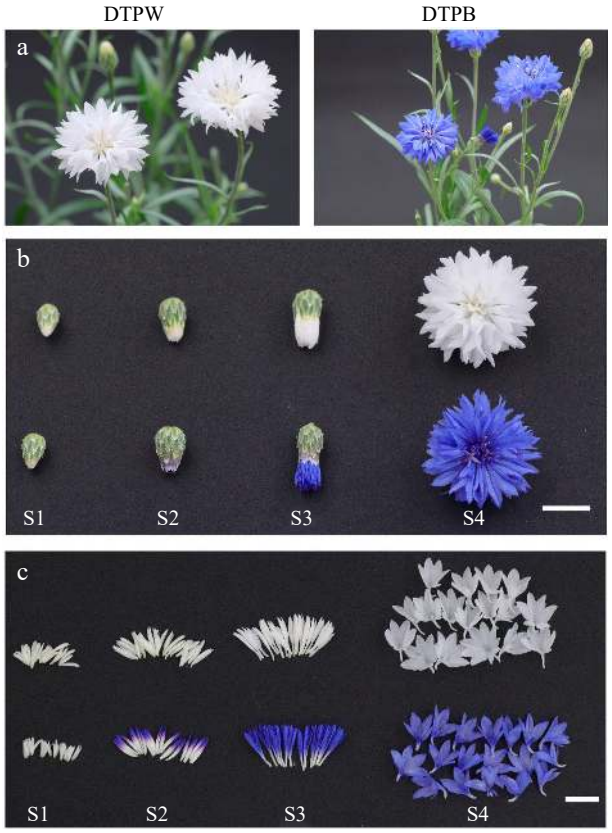


**Fig. 1** Different cultivars and developmental stages of cornflower. (a) Two cornflower cultivars with white and blue petals in DTPW and DTPB, respectively. (b) The capitula were classified into four developmental stages, bar = 1 cm. (c) The pigmentation pattern of cornflower petals in different developmental stages, bar = 1 cm.

qRT-PCR was performed in roots, stems, leaves, sepals, and petals of both DTPW and DTPB using the TB Green® *Premix Ex Taq*™ II (Takara, Japan). Conflower actin (KY621346) was used as the reference gene. All the primers were designed based on the transcriptome database[34] and listed in Supplementary Table S1.

### DNA extraction and isolation of genomic CcbHLH1

The fresh leaves were cut from DTPB in the vegetative period, precooled in liquid nitrogen, and ground into a powder. Then the whole-genome DNA was extracted using the super plant genomic DNA kit according to the instructions (TIANGEN, China). To further explore the genomic structure of CcbHLH1, the PrimeSTAR® Max DNA polymerase (Takara, Japan) was used to amplify its genomic sequence. Furthermore, the purified PCR products were ligated into the pCE3 blunt vector, followed by the transformation into *Escherichia coli* DH5$\alpha$ and sequencing. All the primers are listed in Supplementary Table S1.

### Phylogenetic analysis and sequence alignment

A maximum likelihood phylogenetic tree was constructed by the Jones-Taylor-Thornton (JTT) model using MEGA11. Deduced protein sequences were firstly aligned using MUSCLE, followed by the phylogeny test with 1,000 bootstrap replications. Besides, gaps or missing data were treated as complete deletions.

DNAMAN software was applied to obtain the multi-sequence alignment result.

## Subcellular localization of key genes

The pCAMBIA vector carrying an EGFP was digested with *Nco*I and *Spe*I, followed by the ligation with *CcMYB6-1*, *CcbHLH1* and its mutant without stop codons using homologous recombination. The empty and recombinant plasmids were transformed into *Agrobacterium tumefaciens* GV3101, respectively. GV3101s were resuspended in the liquid mixture containing 10 mM $MgCl_2$, 10 mM MES, and 200 μM acetosyringone, then were adjusted to the $OD_{600}$ of 1, followed by the infiltration into *Nicotiana benthamiana* leaves using needless injections. Before observation, the leaves were immersed in the DAPI (10 μg/mL) for 30 min. Finally, a laser scanning confocal microscope (Leica TCS SP8, Wetzlar, Germany) was used to obtain the fluorescence signal.

## Yeast two-hybrid assay

The restriction endonucleases *Eco*RI and *BamH*I (New England Biolabs) were used to linearize pGBKT7 and pGADT7 empty vectors. The whole length of *CcMYB6-1* was cloned into pGADT7 to form AD-CcMYB6-1 recombinant, while *CcbHLH1* and its mutant were cloned into pGBKT7 to construct BD-CcbHLH1 and BD-CcbHLH1# recombinants. Then, these empty vector and/or recombinant plasmids were co-transformed into Y2H strain by use of yeastmaker™ yeast transformation system 2 (Clontech, USA) and plated on the SD/-Leu/-Trp solid medium, followed by incubation upside down at 30 °C for three days. The matchmaker™ insert check PCR mix 2 (Takara, Japan) was used to ensure the successful insertion of target genes into the yeast strain, followed by the evaluation on the SD/-Trp-Leu-His-Ade medium supplemented with X-$\alpha$-Gal and 3-amino-1,2,4-triazole (3AT).

## Bimolecular luminescence complementary assay

The bimolecular luminescence complementary assay was further conducted to get more evidence of protein-protein interaction between CcMYB6-1, and CcbHLH1, or CcbHLH1#. The empty pCAMBIA1300-cluc (cLUC) and pCAMBIA1300-nluc (nLUC) plasmids were digested with *Kpn*I and *Sal*I for linearization. The full-length sequence of *CcMYB6-1* was ligated into linearized cLUC, while *CcbHLH1* and *CcbHLH1#* without stop codons were cloned into linearized nLUC, respectively. Subsequently, the empty or recombinant plasmids were transformed into *A. tumefaciens* GV3101 severally, followed by the infiltration of GV3101s of different combinations into *N. benthamiana* leaves at an equal volume ratio of cLUC and nLUC. After three days of co-culture in the dark, the D-luciferin potassium salt solution was sprayed on the leaf abaxial surface, followed by the observation of fluorescence signals using a molecular imaging system (LB983 NightOwl II).

## Dual luciferase assay

The promoter region of *CcDFR*, a key structural gene catalyzing anthocyanin biosynthesis, was isolated as in our previous publication[34]. Restriction endonucleases *Kpn*I and *BamH*I (New England Biolabs) were used to digest pGreenII 0800-LUC empty vector in rCutSmart buffer at 37 °C for 15 min, then *CcDFR* promoter of 1,510 bp was cloned into the linearized pGreenII 0800-LUC by homologous recombination. The full-length sequences of *CcMYB6-1*, *CcbHLH1* and *CcbHLH1#* were recombined into pGreenII 62-SK vector. All the recombinants were individually transformed into *A. tumefaciens* GV3101 and verified as a positive clone by polymerase chain reaction. Subsequently, a total of six groups including SK, SK + CcMYB6-1, SK + CcbHLH1, SK + CcbHLH1#, CcMYB6-1 + CcbHLH1, and CcMYB6-1 + CcbHLH1# were individually mixed with LUC-*DFRpro* at a ratio of 10:1 (v:v). The GV3101s containing different recombinants were infiltrated into *N. benthamiana* leaves using a needless injector. After three days of cultivation, the infiltrated leaves were painted with a layer of D-luciferin potassium salt liquid containing 0.1% Triton-x-100, and then photographed using the molecular imaging system (LB983 NightOwl II). Moreover, the firefly luciferase and *Renilla* luciferase were extracted following the instructions of Dual-Luciferase® Reporter Assay System E1910 (Promega, USA), and detected by EnVision (PerkinElmer, USA).

## Transient expression in tobacco leaves

To explore the functional changes before and after CcbHLH1 mutation, *N. benthamiana* were used for transient expression. GV3101s containing mixed plasmids including SK + CcMYB6-1, SK + CcbHLH1, SK + CcbHLH1#, CcMYB6-1 + CcbHLH1, or CcMYB6-1 + CcbHLH1# at a ratio of 1:1 (v:v) was infiltrated into leaves using a needleless injector, followed by cultivation in the dark for three days and photographed after nine days. About 0.1 g infiltrated tobacco leaves were weighed and stored at −80 °C before use.

## Semiquantitative analysis of anthocyanin

Cyanidin-3-*O*-glucoside (Cy3G) was used to obtain the regression equation ($Y = 2.9301X$, $R^2 = 0.9959$) at 525 nm. About 0.1 g of fresh samples were accurately weighed, ground into a powder using a grinding machine, and extracted with 1 mL mixture of methanol : $H_2O$ : formic acid : trifluoroacetic acid = 70:27:2:1 (v : v : v : v) at 4 °C overnight, followed by centrifugation at 12,000 rpm for two minutes. As for leaves, stems and sepals, 500 μL chloroform was added to remove chlorophyll before centrifugation. The liquid supernatant was transferred into new tubes for anthocyanin detection using a spectrophotometer.

## Statistical analysis

Data processing was conducted by use of Excel 2021, and SPSS 20.0 was performed to obtain the significant difference analysis using Ducan's multiple test at 1% level. Origin 2021 was used for visualizing the figures.

# Results

## Anthocyanin is completely absent in both vegetative and reproductive organs of the white cornflower

The previous research on cornflower has clarified that there were pelargonidin derivatives in the pink and red petals as well as cyanidin derivatives in the blue, mauve, and black petals, while no anthocyanin was detected in the white petals using the ultra-performance liquid chromatography coupled with photodiode array and tandem mass spectrometry[3]. Here, we further attempted to detect the anthocyanins in root, stem, leaf, and sepal, besides, the dynamic changes of anthocyanin content were also traced among four developmental stages of petals (Supplementary Fig. S1). There was no anthocyanin in the DTPW petals, which was consistent with our previous

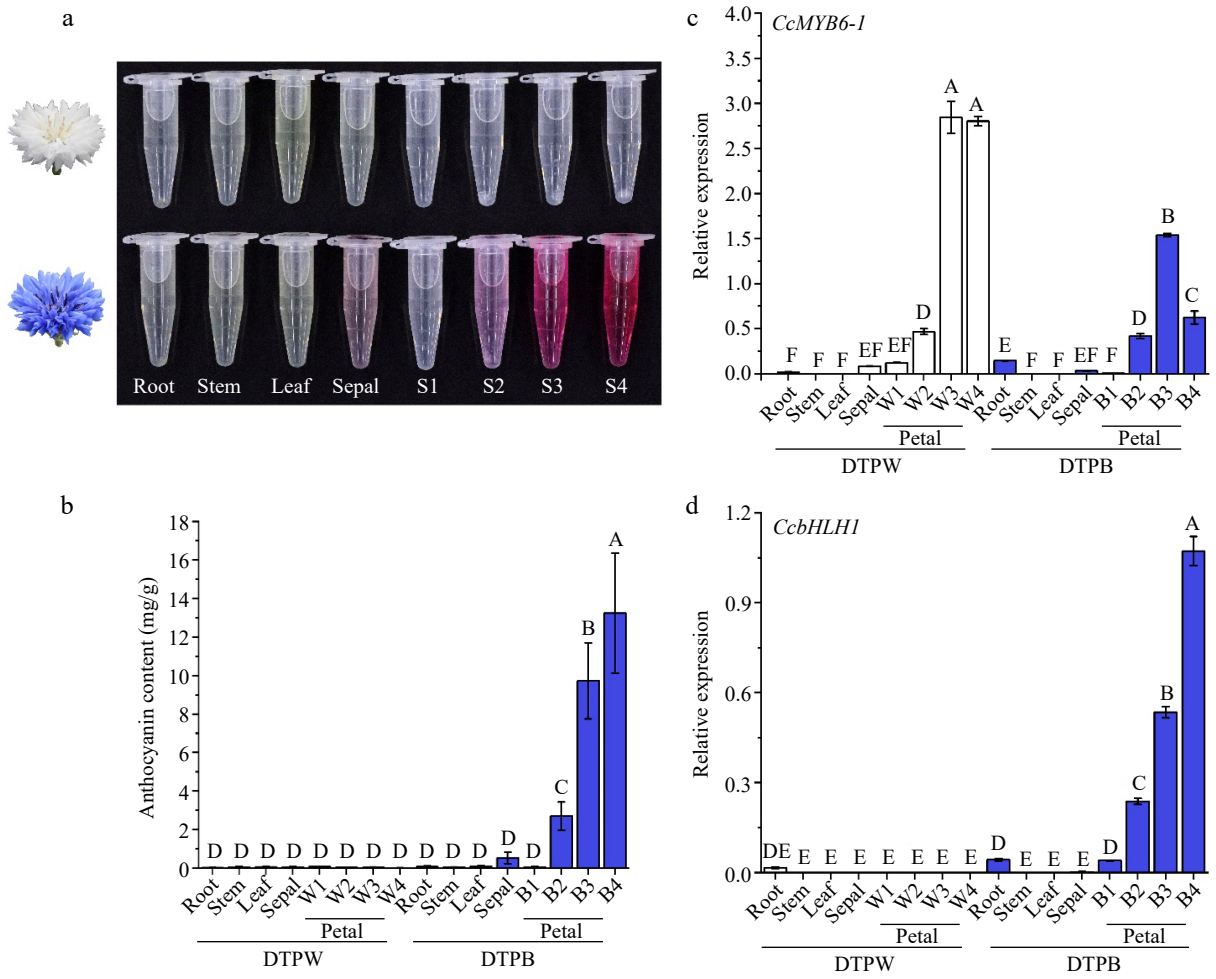


**Fig. 2** Anthocyanins showed specific accumulation in different cultivars and organs of cornflower. (a) The anthocyanin extracts of distinct organs from DTPW and DTPB. (b) Anthocyanin content in different cultivars and organs. Error bars were the S.E. of four biological replicates with each from three individual plantlets. (c), (d) The spatio and temporal expression patterns of *CcMYB6-1* and *CcbHLH1* in DTPW and DTPB. Error bars were the S.E. of three technical replicates. Different capital letters indicate significant difference at 1% level by Duncan's multiple test.

results[3], while the vegetative organs showed no anthocyanin accumulation, either (Fig. 2a & b), suggesting anthocyanins were completely absent in DTPW. Comparatively, the sepals accumulated trace anthocyanins and the anthocyanin contents in petals continuously increased with flower development and peaked at stage four (Fig. 2a & b), suggesting anthocyanins accumulated in both sepals and petals of DTPB.

The expression pattern of structural genes was further analyzed including *CcF3H*, *CcF3'H*, *CcDFR*, *CcANS*, *CcGT*, and *CcAT* in the spatio levels to clarify the potential mechanism of anthocyanin absence in DTPW (Supplementary Fig. S2). Notably, the *CcDFR* was specifically expressed in the reproductive period. All the biosynthetic genes in the blue petals were significantly higher expressed than others, while the white petals only showed a tiny amount of gene expression, which were consistent with our previous publication[3]. These results suggested that the down-regulating of biosynthetic gene expression accounted for the anthocyanin absence in DTPW. Our previous research identified two transcription factors (TFs) positively regulating anthocyanin biosynthesis in cornflower, namely CcMYB6-1 and CcbHLH1[34]. The qRT-PCR results revealed that the white petals showed significantly higher expression of *CcMYB6-1* (Fig. 2c), while the *CcbHLH1* transcript was nearly undetectable in DTPW (Fig. 2d), indicating *CcbHLH1* may be responsible for the down-regulating of biosynthetic genes in DTPW.

## A spontaneous mutation of CcbHLH1 occurs in the white cornflower petals

Further, an attempt was made to isolate the full-length sequences of those two TFs using the cDNA library constructed from the petals of both DTPW and DTPB. Firstly, a polymerase chain reaction was performed to amplify the whole length of two TFs using primers based on the published sequence information in the blue cornflower cultivar DTPB. The agarose gel electrophoresis showed that *CcMYB6-1* could be successfully amplified in DTPW (Supplementary Fig. S3a), and its sequence contained the whole R2 and R3 domains, 100% consistent with that in DTPB (Fig. 3a), suggesting CcMYB6-1 was not the main cause for anthocyanin absence in DTPW. Then, three pairs of primers were designed to amplify different fragments of *CcbHLH1* (Supplementary Fig. S3b), and the agarose gel electrophoresis showed that there were clear bands of fragment 1 and fragment 2, however, fragment 3 could only be amplified in DTPB (Supplementary Fig. S3c), suggesting its full-length was

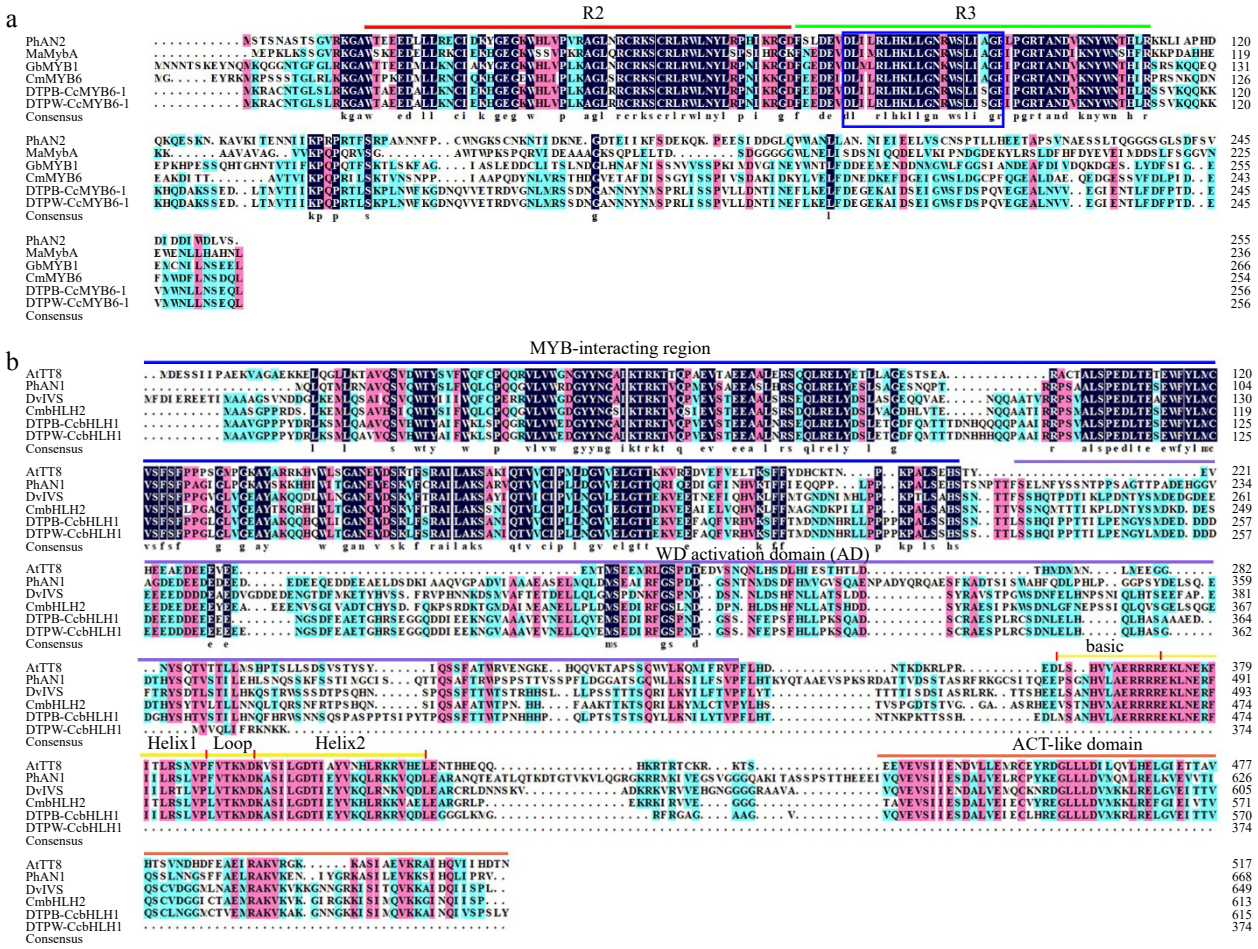


**Fig. 3** Amino acid sequence alignment of MYBs and bHLHs regulating anthocyanin biosynthesis in different species. (a) Protein sequence alignment of MYBs with the conserved R2 and R3 domains marked in red and green lines, respectively. The blue rectangle indicated conserved motif of [D/E]LX2[K/R]X3LX6LX3R. PhAN2 (*P.* × *hybrida*, AAF66727), MaMybA (*Muscari armeniacum*, AVD68967), GbMYB1 (*Gynura bicolor*, BAJ17661), CmMYB6 (*Chrysanthemum* × *morifolium*, AKP06190). (b) Protein sequence alignment of bHLHs. The MYB-interacting region, WD activation, bHLH, and ACT-like domains were marked with lines in different colors. AtTT8 (*A. thaliana*, CAC14865), PhAN1 (*P.* × *hybrida*, AAG25927), DvIVS (*D. variabilis*, BAJ33515), and CmbHLH2 (*C.* × *morifolium*, ALR72603).

possibly missing in the white petals. Then 3' RACE was performed to obtain the whole length of *CcbHLH1* in DTPW. Finally, a sequence with 1,125 base pairs was joined and further verified by amplification using high-fidelity enzyme. The multi-sequence alignment analysis showed that the truncated CcbHLH1 in DTPW lost partial WD activation domain, the whole basic helix-loop-helix domain in the N-terminal, and the aspartokinase, chorismite mutase, TyrA (ACT)-like domain in the C-terminal (Fig. 3b). For convenience, the truncated *CcbHLH1* was renamed as *CcbHLH1#* in the following assays. These results revealed that a naturally spontaneous mutation of *CcbHLH1* occurred in DTPW, which may account for its anthocyanin absence.

## Alternative splicing is responsible for the truncation of CcbHLH1

The qRT-PCR results revealed that *CcbHLH1#* was specifically expressed in the petals, and its abundance in the white petals was significantly higher than that in the blue petals ($p < 0.01$) (Fig. 4a). To further explore the molecular mechanism underlying the truncation of *CcbHLH1*, its genomic sequence was isolated in DTPB, which contained four exons and three introns (Fig. 4b). The mature mRNA of *CcbHLH1* consisted of four complete exons, carrying the key basic, helix-loop-helix domain (Fig. 4b). Comparatively, the *CcbHLH1#* transcript consisted of exons 1, 2, and partial retention of intron 2, losing the key bHLH domain (Fig. 4b). Furthermore, phylogenetic analysis of the predicted amino acid sequences of CcbHLH1 and CcbHLH1# with other bHLHs that regulate flavonoid biosynthesis in other species revealed they belong to the bHLH2 clade within the IIIf subgroup (Fig. 4c).

## The subcellular localization analysis of CcbHLH1

To further clarify if the functional position changed after *CcbHLH1* truncation, the subcellular analysis was conducted using GFP as a reporter gene, whose transcription was activated by the constitutive CaMV 35S promoter. The *CcMYB6-1*, *CcbHLH1*, and *CcbHLH1#* without stop codons were successfully fused with GFP. There were strong GFP fluorescence signals widely found in the whole cell transformed with an empty vector. Comparatively, the GFP fluorescence signals of *CcMYB6-1*, and *CcbHLH1* were mainly focused in the nucleus (Fig. 5), which was consistent with our previous identification that *CcMYB6-1* and *CcbHLH1* functioned as transcription factors

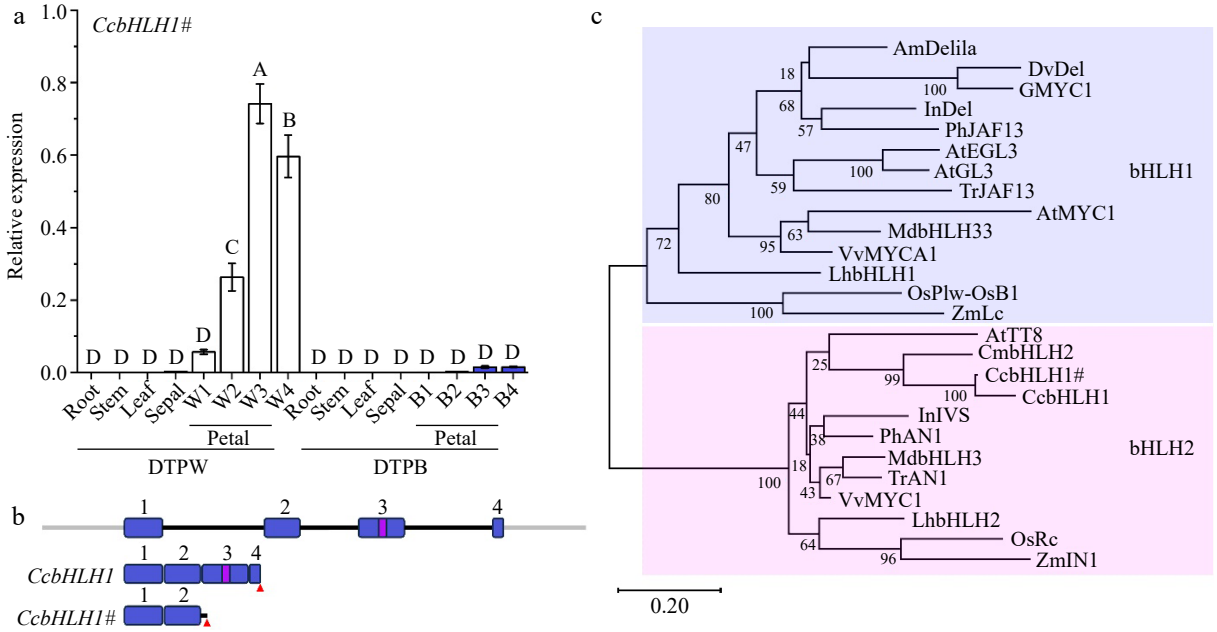


**Fig. 4** Molecular and phylogenetic analysis of CcbHLH1 and CcbHLH1#. (a) The spatio and temporal expression patterns of *CcbHLH1#* in DTPW and DTPB. Error bars were the S.E. of three technical replicates. Different capital letters indicate significant difference at 1% level by Duncan's multiple test. (b) Structure of CcbHLH1 and CcbHLH1# genes. Exons are numbered in blue rectangles, introns are indicated by black lines, the bHLH domain is indicated in a violet rectangle, and the red triangle represents stop codon. (c) Phylogenetic tree of subgroup IIIf bHLHs. AmDelila (*A. majus*, AAA32663.1), DvDel (*D. pinnata*, BAJ33516.1), GMYC1 (*Gerbera hybrid*, CAA07615.1), InDel (*I. nil*, XP_019171149.1), PhJAF13 (*P.* × *hybrida*, AAC39455.1), AtEGL3 (*A. thaliana*, OAP12509.1), AtGL3 (*A. thaliana*, NP_680372.1), TrJAF13 (*Trifolium repens*, AIT76563.1), AtMYC1 (*A. thaliana*, NP_001154194), MdbHLH3 (*Malus domestica*, ADL36597.1), MdbHLH33 (*M. domestica*, ABB84474.1), VvMYCA1 (*Vitis vinifera*, NP_001267954.1), LhbHLH1 (*Lilium hybrida*, BAE20057.1), LhbHLH2 (*L. hybrida*, BAE20058.1), OsPlw-OsB1 (*Oryza sativa*, BAB64301.1), ZmLc (*Zea mays*, AAA33504.1), AtTT8 (*A. thaliana*, Q9FT81), CmbHLH2 (*C.* × *morifolium*, ALR72603.1), InIVS (*I. nil*, XP_019197480.1), PhAN1 (*P.* × *hybrida*, AAG25928.1), TrAN1 (*T. repens*, AIT76559.1), VvMYC1 (*V. vinifera*, NP_001268182.1), OsRc (*O. sativa*, ADK36625.1), ZmIN1 (*Z. mays*, AAB03841.1).

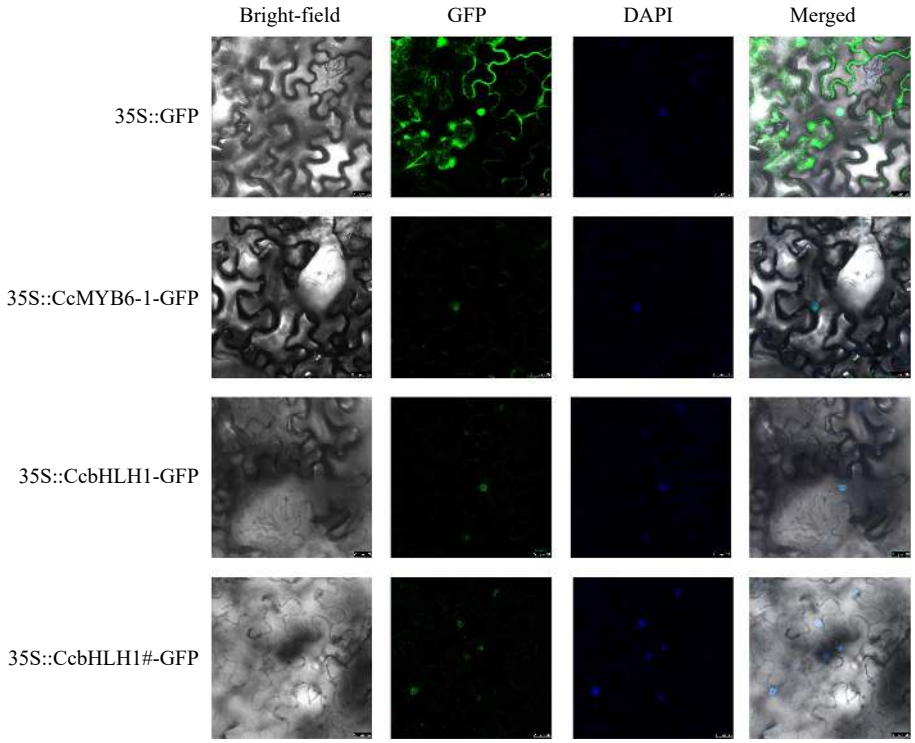


**Fig. 5** The subcellular localization analysis of CcMYB6-1, CcbHLH1, and CcbHLH1#. DAPI was used as a nuclear-localized marker. Photos were captured two days after infiltration.

synergistically involved in regulating anthocyanin biosynthesis in cornflower[34]. Similarly, the green fluorescence signals of *CcbHLH1#* were also observed in the nucleus (Fig. 5), suggesting the loss of multi-domains didn't change its functional position.

## CcbHLH1# remains the protein-protein interaction with CcMYB6-1

The yeast two-hybrid assay was conducted to explore whether the protein-protein interaction relationship changed between the truncated CcbHLH1 and CcMYB6-1. Yeast transformed with pGBKT7-53 and pGADT7-T as well as pGBKT7-lam and pGADT7-T were designed for the positive and negative control, respectively. A total of five combinations were performed, and all of them could grow well on the SD/-Trp-Leu plate, suggesting all the target plasmids were successfully transformed into the Y2HGold yeast strain (Fig. 6a). The following observation found that yeast transformed with BD-CcbHLH1/CcbHLH1# and empty AD or empty BD and AD-CcMYB6-1 could not grow on the SD/-Trp-Leu-His-Ade+X-$\alpha$-gal + 3AT plate, similar as the negative control. Comparatively, yeast co-transformed with CcMYB6-1 and CcbHLH1 or CcbHLH1# grew well and exhibited significant blue color on the same medium, similar as the positive control (Fig. 6a). Moreover, the bimolecular luminescence complementary assay was also conducted to obtain more evidence. There was no fluorescence signal detected in the combinations of nLUC + cLUC, nLUC + cLUC-CcMYB6-1, and nLUC-CcbHLH1/CcbHLH1# + cLUC, while significantly stronger fluorescence signals were found both in the nLUC-CcbHLH1 + cLUC-CcMYB6-1 and nLUC-CcbHLH1# + cLUC-CcMYB6-1, further verifying the protein-protein interaction between CcbHLH1/CcbHLH1# and CcMYB6-1 (Fig. 6b). These results indicated that the truncation of CcbHLH1 didn't change its protein interaction with CcMYB6-1.

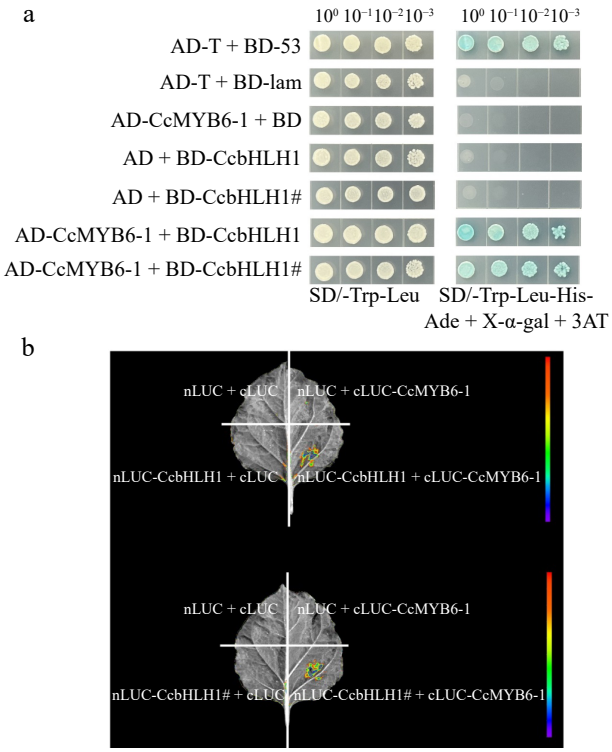


**Fig. 6** Protein-protein interaction before and after CcbHLH1 mutation with CcMYB6-1. (a) Y2H strain transformed with targeted plasmids were plated on the SD/-Trp-Leu (left) and SD/-Trp-Leu-His-Ade + X-$\alpha$-gal + 3AT (right) solid medium. (b) The firefly fluorescence of tobacco leaves injected with different combinations of targeted genes.

## CcbHLH1# loses the ability to enhance the trans-activation of *CcDFR* promoter

A previous study indicated that CcMYB6-1 could trans-activate the promoters of structural genes involved in anthocyanin biosynthesis and this trans-activation was significantly enhanced when co-expressed with CcbHLH1[34]. The late anthocyanin biosynthetic gene *CcDFR* was then chosen to clarify whether the mutational CcbHLH1 could retain the ability to enhance gene expression. Firstly, tobacco leaves were infiltrated with CcbHLH1, CcbHLH1#, and CcMYB6-1, respectively, followed by the visualization of firefly fluorescence using a molecular imaging system. The fluorescence signal in CcMYB6-1 was significantly stronger than that in the CcbHLH1/CcbHLH1#, suggesting CcbHLH1 or its mutant alone could not trans-activate the *CcDFR* promoter (Supplementary Fig. S4). Then CcbHLH1 and CcMYB6-1 were co-expressed and more stronger fluorescence signal was obtained, however, the signal in CcbHLH1# + CcMYB6-1 was similar as that in the SK + CcMYB6-1, suggesting CcbHLH1# could not enhance the trans-activation of the *CcDFR* promoter (Fig. 7a). Moreover, the dual luciferase assay was conducted to obtain more concrete statistics. The value of LUC/REN in SK was set as 1 for convenience. The combinations of SK + CcbHLH1/CcbHLH1# could not up-regulate the activity of *CcDFR* promoter, which was consistent with the molecular imaging results. Comparatively, co-transformed CcMYB6-1 and CcbHLH1 significantly enhanced the activity of the *CcDFR* promoter with 12.9-fold induction, while there was no significant difference between CcMYB6-1 + CcbHLH1# and SK + CcMYB6-1 ($p < 0.01$) (Fig. 7b). These results indicated that the truncated CcbHLH1 lost the ability to enhance the trans-activation of *CcDFR* promoter, which possibly was the main reason for the anthocyanin absence in DTPW.

## Anthocyanin content in tobacco leaves decreases after CcbHLH1 mutation

Due to the lack of a stable genetic transformation system, the transient over-expression in tobacco leaves were conducted to clarify the functional changes after CcbHLH1 mutation. A total of five combinations were designed, including SK + CcMYB6-1, SK + CcbHLH1, SK + CcbHLH1#, CcMYB6-1 + CcbHLH1, and CcMYB6-1 + CcbHLH1#. After 9 d of co-cultivation, tobacco leaves infiltrated with CcMYB6-1 turned green to red, in which the CcMYB6-1 + CcbHLH1 group exhibited the darkest red, followed by CcMYB6-1 + CcbHLH1#, and SK + CcMYB6-1 groups. On the contrary, tobacco leaves infiltrated with SK + CcbHLH1 or SK + CcbHLH1# retained green (Fig. 8a). These results indicated that only CcMYB6-1 expressed can the tobacco leaves turn red, which was consistent with our previous research[34]. Notably, the leaves exhibited pale red rather than darker red after CcbHLH1 mutation, suggesting its function of synergistically regulating anthocyanin biosynthesis with CcMYB6-1 was also missing. Furthermore, the semi-quantitative interpretation using Cy3G as a standard was performed to obtain more direct evidence. There was no anthocyanin detected in SK + CcbHLH1 and SK + CcbHLH1# groups, while the anthocyanin content in CcMYB6-1 + CcbHLH1 was 10.8 mg/g

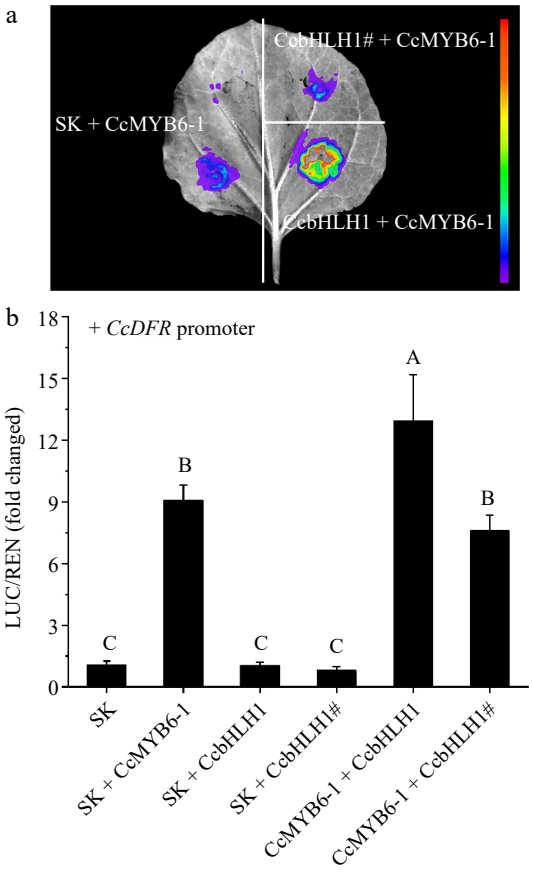


**Fig. 7** Changes of trans-activation of *CcDFR* promoter before and after CcbHLH1 mutation. (a) The firefly fluorescence captured by a molecular imaging system after three days infiltration. (b) *In vivo* interactions between CcMYB6-1, CcbHLH1, and its mutant CcbHLH1# on the *CcDFR* promoter. Error bars were the S.E. of three biological replicates with each from at least two individual leaves. Different capital letters indicate significant difference at 1% level by Duncan's multiple test.

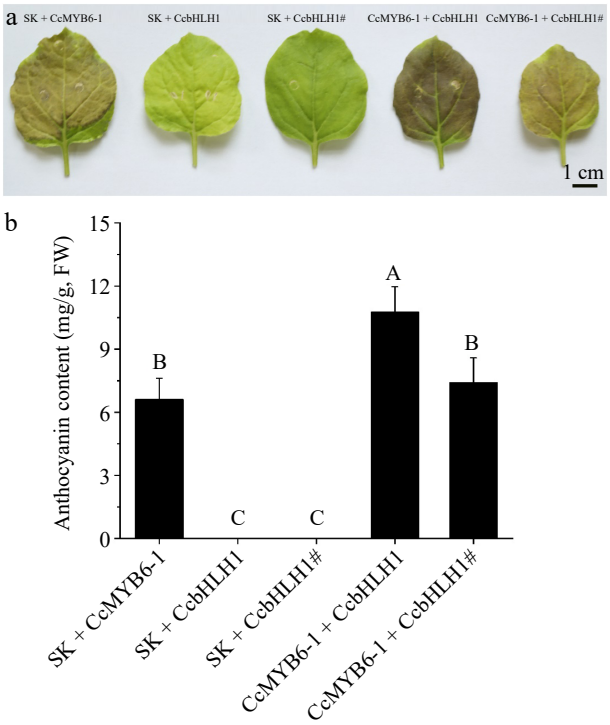


**Fig. 8** Transient over-expression in tobacco leaves. (a) Tobacco leaves infiltrated with five different combinations including SK + CcMYB6-1, SK + CcbHLH1, SK + CcbHLH1#, CcMYB6-1 + CcbHLH1, and CcMYB6-1 + CcbHLH1#. The photo was captured 9 d after infiltration. (b) The semi-quantification of anthocyanin accumulating in tobacco leaves. Error bars were the S.E. of four biological replicates with each from at least two individual leaves. Different capital letters indicate significant difference at 1% level by Duncan's multiple test.

(fresh weight, FW), significantly higher than that in other combinations. Notably, there was no significant difference between SK + CcMYB6-1 and CcMYB6-1 + CcbHLH1# ($p < 0.01$) (Fig. 8b), suggesting the truncated CcbHLH1 didn't play a role in stimulating anthocyanin biosynthesis together with CcMYB6-1. These results revealed that the loss of the conserved multi-domains of CcbHLH1 led to the loss of the ability to up-regulate anthocyanin biosynthesis with CcMYB6-1, which can account for the anthocyanin absence in the white petals of cornflower.

## Discussion

Cornflower is favored by its exquisite capitulum and abundant flower color variation thereby is widely used in garden design, cut flowers, and food decoration. In our previous study, six cornflower cultivars with pure colors were collected. The UPLC-MS/MS analysis revealed that pelargonidin and cyanidin derivatives were the main anthocyanins accumulating in the pink/red and blue/mauve/black petals, respectively, while there was no anthocyanin detected in the white cornflower petals, which only accumulated apigenin derivatives[3]. Here, anthocyanins were further monitored in both vegetative and reproductive organs of cornflower (Fig. 2). There was no anthocyanin detected in roots, stems, and leaves, suggesting the anthocyanin deficiency in vegetative organs of cornflower. Notably, anthocyanins accumulated slightly in the sepals, and increased with petal development in DTPB, while no anthocyanin was found in both sepals and petals of DTPW, indicating its complete anthocyanin absence, which was further explained by the block of structural genes including *CcF3'H*, *CcDFR*, *CcGT*, and *CcAT* (Supplementary Fig. S2).

To date, CcMYB6-1 and CcbHLH1 have been functionally characterized as positive regulators involved in the anthocyanin biosynthesis in cornflower. Considering that MYBs mutation usually leads to the anthocyanin deficiency and white phenotype in *Raphanus sativus* taproots, grapes, strawberries, and citrus[35–38], we focused on the gene expression and sequence isolation of *CcMYB6-1*. Unexpectedly, the transcript level of *CcMYB6-1* was significantly higher in DTPW petals ($p < 0.01$, Fig. 2), and its full-length sequence in DTPW was entirely consistent with that in DTPB (Fig. 3), which was distinct from the *CgsMYB12* mutation caused by a 1-bp deletion in the white basal region of *Clarkia gracilis*[39], the *FaMYB10* mutation caused by an AG insertion in the white-fleshed strawberry[37], as well as the *LsTT2* mutation in the white seeds of lettuce[40]. Notably, *CcbHLH1* transcript was undetectable in DTPW (Fig. 2), consistent with the absence of structural gene expression and anthocyanin accumulation. The following gene isolation and

multi-sequence alignment showed that *CcbHLH1* in the white cornflower was spontaneously truncated to 1,125 bp, losing the basic helix-loop-helix domain in the N-terminal and the ACT-like domain in the C-terminal (Fig. 3), two necessary domains in regulatory activity, the mutation of which usually results in anthocyanin decrease[41,42].

Generally, the base deletion or insertion, transposon insertion, and alternative splicing will give rise to the premature stop codon and frameshift, finally leading to the truncation of coding genes and anthocyanin loss[43–48]. In this study, the truncation of *CcbHLH1* is the result of alternative splicing by comparing the genome sequence with two transcripts (Fig. 4). The truncated CcbHLH1# protein is still localized in the nucleus and could interact with CcMYB6-1 (Figs 5 & 6), suggesting the loss of necessary domains doesn't change its functional position and interaction relationship, which may be explained by the invariant MYB-interaction region in the N-terminal[18]. The following dual-luciferase assay revealed that CcbHLH1 alone couldn't stimulate the trans-activity of the *CcDFR* promoter, suggesting its function in a CcMYB6-1-dependent way (Fig. 7), which was different from petunia anthocyanin1, also a bHLH2 clade TF, that directly activates the expression of the *dfrA* gene[27]. However, the enhanced trans-activation of *CcDFR* promoter and anthocyanin biosynthesis ability when co-expressed with CcMYB6-1 disappeared after CcbHLH1 truncation (Figs 7 & 8), suggesting the loss of basic helix-loop-helix domain and ACT-like domain contributed to the regulatory inactivation, similar to the cases in chrysanthemum, tomato and petunia[29,49,50].

A possible explanation is that the truncated TFs function as inhibitors involved in either competing with the functional protein for activation sites of structural genes or the formation of effective MYB-bHLH-WD40 protein complex, thus significantly affects anthocyanin levels. In maize, the dominant mutant C1-I, a truncated MYB transcription factor acts as anthocyanin inhibitor by competing C1 for activator sites of the biosynthetic genes like *R1-nj*[51]. Truncated MYBs or bHLHs usually lose the original ability to form the MBW complex thus leading to the anthocyanin decrease and color fading like chrysanthemum, radish, and wheat[29,52,53]. Differently, the truncated CcbHLH1 of cornflower retains its interaction with CcMYB6-1, but this CcbHLH1#-CcMYB6-1 complex can't effectively enhance the trans-activity of *CcDFR* promoter and anthocyanin accumulation in tobacco leaves like CcbHLH1-CcMYB6-1 complex (Figs 7 & 8), suggesting that the truncated variant inhibits anthocyanin biosynthesis by forming a dysfunctional complex.

Alternative splicing plays a key regulatory role in anthocyanin accumulation, leading to the color variation of higher plant organs. The anthocyanin-free phenotype of the eggplant *efc1* mutant is caused by the retention of the second intron in *DFR* by improper splicing[54]. In tomato and *Brassica napus*, alternative splicing brings the truncated R2R3-MYB protein without the key R3 domain, resulting in the non-interaction with bHLH transcription factor, and finally leading to anthocyanin loss[55,56]. Interestingly, there are three kinds of splicing variants of bHLH2 in chrysanthemum, namely, the activator CmbHLH2 with complete domains and the strongest regulatory effect, the activator CmbHLH2.1 with 26 amino acids difference at the C-terminal and less regulatory effect, as well as the dysfunctional CmbHLH2$^{short}$ with only partial MIR domain at the N-terminal[24,29,30], suggesting the more domains lost, the more functions disappear. The missing multi-domains in cornflower CcbHLH1# is also caused by alternative splicing, leading to the complete anthocyanin loss in DTPW. Together, these findings reveal alternative splicing may play a potential role in modulating anthocyanin biosynthesis in cornflower. The regulatory mechanism underlying alternative splicing remains to be seen in the near future.

## Conclusions

The transcription activator in cornflower, *CcbHLH1*, was truncated to 1,125 bp because of alternative splicing, losing multi-domains at the C-terminal. The mutated CcbHLH1 protein could interact with CcMYB6-1, but lose the ability to trans-activate promoter activity of anthocyanin biosynthetic genes and to induce anthocyanin biosynthesis thereby, which resulted in the complete anthocyanin absence in the white cornflower. These obtained results provide insights into the molecular mechanism underlying the white color transition in higher plants.

## Author contributions

The authors confirm contribution to the paper as follows: study conception and design: Deng C, Dai S; data collection and analysis: Deng C, Zheng X, Wang J, Li Y, Li J, Lu M, Gao R, Ji C, Hao Q; draft manuscript preparation: Deng C, Zheng X, Wang J, Li Y, Li J, Lu M, Gao R, Ji C, Hao Q. All authors reviewed the results and approved the final version of the manuscript.

## Data availability

All data generated or analyzed during this study are included in this published article and its supplementary information files.

## Acknowledgments

This research was supported by the National Natural Science Foundation, China (No. 32101579 and 32171849), the Shandong Province Natural Science Foundation, China (No. ZR2021QC143) and Shandong students' project for innovation training (S202210452029).

## Conflict of interest

The authors declare that they have no conflict of interest.

**Supplementary information** accompanies this paper at (https://www.maxapress.com/article/doi/10.48130/opr-0024-0028)

## Dates

Received 5 March 2024; Revised 10 September 2024; Accepted 21 October 2024; Published online 21 November 2024

## References

1. Rudall PJ. 2020. Colourful cones: how did flower colour first evolve? *Journal of Experimental Botany* 71(3):759–67

2. Kellenberger RT, Glover BJ. 2023. The evolution of flower colour. *Current Biology* 33:R484–R488
3. Deng C, Li S, Feng C, Hong Y, Huang H, et al. 2019. Metabolite and gene expression analysis reveal the molecular mechanism for petal colour variation in six *Centaurea cyanus* cultivars. *Plant Physiology and Biochemistry* 142:22–33
4. Guo F, Guan R, Sun X, Zhang C, Shan C, et al. 2023. Integrated metabolome and transcriptome analyses of anthocyanin biosynthesis reveal key candidate genes involved in colour variation of *Scutellaria baicalensis* flowers. *BMC Plant Biology* 23:643
5. Ai Y, Zheng QD, Wang MJ, Xiong LW, Li P, et al. 2023. Molecular mechanism of different flower color formation of *Cymbidium ensifolium*. *Plant Molecular Biology* 113:193–204
6. Tanaka Y, Sasaki N, Ohmiya A. 2008. Biosynthesis of plant pigments: anthocyanins, betalains and carotenoids. *The Plant Journal* 54:733–49
7. Saigo T, Wang T, Watanabe M, Tohge T. 2020. Diversity of anthocyanin and proanthocyanin biosynthesis in land plants. *Current Opinion in Plant Biology* 55:93–99
8. Fukada-Tanaka S, Hoshino A, Hisatomi Y, Habu Y, Hasebe M, et al. 1997. Identification of new *Chalcone* synthase genes for flower pigmentation in the Japanese and common morning glories. *Plant and Cell Physiology* 38(6):754–58
9. Nishihara M, Yamada E, Saito M, Fujita K, Takahashi H, et al. 2014. Molecular characterization of mutations in white-flowered torenia plants. *BMC Plant Biology* 14:86
10. Ohno S, Hosokawa M, Kojima M, Kitamura Y, Hoshino A, et al. 2011. Simultaneous post-transcriptional gene silencing of two different chalcone synthase genes resulting in pure white flowers in the octoploid dahlia. *Planta* 234:945–58
11. Nakatsuka T, Mishiba KI, Abe Y, Kubota A, Kakizaki Y, et al. 2008. Flower color modification of gentian plants by RNAi-mediated gene silencing. *Plant Biotechnology* 25:61–68
12. Ohta Y, Atsumi G, Yoshida C, Takahashi S, Shimizu M, et al. 2022. Post-transcriptional gene silencing of the chalcone synthase gene *CHS* causes Corolla lobe-specific whiting of Japanese gentian. *Planta* 255:29
13. Zhou Z, Ying Z, Wu Z, Yang Y, Fu S, et al. 2021. Anthocyanin genes involved in the flower coloration mechanisms of *Cymbidium kanran*. *Frontiers in Plant Science* 12:737815
14. Lin C, Xing P, Jin H, Zhou C, Li X, et al. 2022. Loss of anthocyanidin synthase gene is associated with white flowers of *Salvia miltiorrhiza* Bge. f. alba, a natural variant of *S. miltiorrhiza*. *Planta* 256:15
15. Gould B, Kramer EM. 2007. Virus-induced gene silencing as a tool for functional analyses in the emerging model plant *Aquilegia* (Columbine, Ranunculaceae). *Plant Methods* 3:6
16. Xue L, Wang J, Zhao J, Zheng Y, Wang HF, et al. 2019. Study on cyanidin metabolism in petals of pink-flowered strawberry based on transcriptome sequencing and metabolite analysis. *BMC Plant Biology* 19:423
17. Ma L, Zhang Y, Cui G, Duan Q, Jia W, et al. 2023. Transcriptome analysis of key genes involved in color variation between blue and white flowers of *Iris bulleyana*. *BioMed Research International* 2023:7407772
18. Hichri I, Barrieu F, Bogs J, Kappel C, Delrot S, et al. 2011. Recent advances in the transcriptional regulation of the flavonoid biosynthetic pathway. *Journal of Experimental Botany* 62(8):2465–83
19. Cappellini F, Marinelli A, Toccaceli M, Tonelli C, Petroni K. 2021. Anthocyanins: from mechanisms of regulation in plants to health benefits in foods. *Frontiers in Plant Science* 12:748049
20. Schwinn K, Venail J, Shang Y, MacKay S, Alm V, et al. 2006. A small family of *MYB*-regulatory genes controls floral pigmentation intensity and patterning in the genus *Antirrhinum*. *The Plant Cell* 18:831–51
21. Hoballah ME, Gübitz T, Stuurman J, Broger L, Barone M, et al. 2007. Single gene–mediated shift in pollinator attraction in *Petunia*. *The Plant Cell* 19:779–90
22. Gates DJ, Olson BJSC, Clemente TE, Smith SD. 2018. A novel R3 MYB transcriptional repressor associated with the loss of floral pigmentation in *Iochroma*. *New Phytologist* 217:1346–56
23. Zhu HF, Fitzsimmons K, Khandelwal A, Kranz RG. 2009. CPC, a single-repeat R3 MYB, is a negative regulator of anthocyanin biosynthesis in *Arabidopsis*. *Molecular Plant* 2(4):790–802
24. Xiang L, Liu X, Li H, Yin X, Grierson D, et al. 2019. *CmMYB#7*, an R3 MYB transcription factor, acts as a negative regulator of anthocyanin biosynthesis in chrysanthemum. *Journal of Experimental Botany* 70(12):3111–23
25. He J, Xu Y, Huang D, Fu J, Liu Z, et al. 2022. TRIPTYCHON-LIKE regulates aspects of both fruit flavor and color in citrus. *Journal of Experimental Botany* 73(11):3610–24
26. Feller A, Machemer K, Braun EL, Grotewold E. 2011. Evolutionary and comparative analysis of MYB and bHLH plant transcription factors. *The Plant Journal* 66:94–116
27. Spelt C, Quattrocchio F, Mol JNM, Koes R. 2000. *anthocyanin1* of Petunia encodes a basic helix-loop-helix protein that directly activates transcription of structural anthocyanin genes. *The Plant Cell* 12:1619–31
28. Park KI, Ishikawa N, Morita Y, Choi JD, Hoshino A, et al. 2007. A *bHLH* regulatory gene in the common morning glory, *Ipomoea purpurea*, controls anthocyanin biosynthesis in flowers, proanthocyanidin and phytomelanin pigmentation in seeds, and seed trichome formation. *The Plant Journal* 49:641–54
29. Lim SH, Kim DH, Jung JA, Lee JY. 2021. Alternative splicing of the basic helix–loop–helix transcription factor gene *CmbHLH2* affects anthocyanin biosynthesis in Ray florets of Chrysanthemum (*Chrysanthemum morifolium*). *Frontiers in Plant Science* 12:669315
30. Xiang L, Liu X, Shi Y, Li Y, Li W, et al. 2021. Comparative transcriptome analysis revealed two alternative splicing bHLHs account for flower color alteration in chrysanthemum. *International Journal of Molecular Sciences* 22:12769
31. Gonzalez A, Zhao M, Leavitt JM, Lloyd AM. 2008. Regulation of the anthocyanin biosynthetic pathway by the TTG1/bHLH/Myb transcriptional complex in Arabidopsis seedlings. *The Plant Journal* 53:814–27
32. Goodrich J, Carpenter R, Coen ES. 1992. A common gene regulates pigmentation pattern in diverse plant species. *Cell* 68:955–64
33. Albert NW, Butelli E, Moss SMA, Piazza P, Waite CN, et al. 2021. Discrete bHLH transcription factors play functionally overlapping roles in pigmentation patterning in flowers of *Antirrhinum majus*. *New Phytologist* 231:849–63
34. Deng C, Wang J, Lu C, Li Y, Kong D, et al. 2020. *CcMYB6-1* and *CcbHLH1*, two novel transcription factors synergistically involved in regulating anthocyanin biosynthesis in cornflower. *Plant Physiology and Biochemistry* 151:271–83
35. Kim DH, Lee J, Rhee J, Lee JY, Lim SH. 2021. Loss of the R2R3 MYB transcription factor RsMYB1 shapes anthocyanin biosynthesis and accumulation in *Raphanus sativus*. *International Journal of Molecular Sciences* 22:10927
36. Walker AR, Lee E, Bogs J, McDavid DAJ, Thomas MR, et al. 2007. White grapes arose through the mutation of two similar and adjacent regulatory genes. *The Plant Journal* 49:772–85
37. Yuan H, Cai W, Chen X, Pang F, Wang J, et al. 2022. Heterozygous frameshift mutation in *FaMYB10* is responsible for the natural formation of red and white-fleshed strawberry (*Fragaria* × *ananassa* Duch). *Frontiers in Plant Science* 13:1027567
38. Butelli E, Garcia-Lor A, Licciardello C, Las Casas G, Hill L, et al. 2017. Changes in anthocyanin production during domestication of *Citrus*. *Plant Physiology* 173:2225–42
39. Lin RC, Rausher MD. 2021. *R2R3-MYB* genes control petal pigmentation patterning in *Clarkia gracilis* ssp. *sonomensis* (Onagraceae). *New Phytologist* 229:1147–62
40. Zhang X, Liang X, He S, Tian H, Liu W, et al. 2023. Seed color in lettuce is determined by the *LsTT2*, *LsCHS*, and *Ls2OGD* genes from

the flavonoid biosynthesis pathway. *Theoretical and Applied Genetics* 136:241

41. Feller A, Hernandez JM, Grotewold E. 2006. An ACT-like domain participates in the dimerization of several plant basic-helix-loop-helix transcription factors. *The Journal of Biological Chemistry* 281:28964–74
42. Kong Q, Pattanaik S, Feller A, Werkman JR, Chai C, et al. 2012. Regulatory switch enforced by basic helix-loop-helix and ACT-domain mediated dimerizations of the maize transcription factor R. *Proceedings of the National Academy of Sciences of the United States of America* 109:E2091–E2097
43. He Y, Li S, Dong Y, Zhang X, Li D, et al. 2022. Fine mapping and characterization of the dominant gene *SmFTSH10* conferring non-photosensitivity in eggplant (*Solanum melongena* L.). *Theoretical and Applied Genetics* 135:2187–96
44. Zhang Y, Feng X, Liu Y, Zhou F, Zhu P. 2022. A single-base insertion in *BoDFR1* results in loss of anthocyanins in green-leaved ornamental kale. *Theoretical and Applied Genetics* 135:1855–65
45. Gonda I, Abu-Abied M, Adler C, Milavski R, Tal O, et al. 2023. Two independent loss-of-function mutations in *anthocyanidin synthase* homeologous genes are responsible for the all-green phenotype of sweet basil. *Physiologia Plantarum* 175:e13870
46. Xu ZS, Yang QQ, Feng K, Xiong AS. 2019. Changing carrot color: insertions in *DcMYB7* alter the regulation of anthocyanin biosynthesis and modification. *Plant Physiology* 181:195–207
47. Wang J, Xu R, Qiu S, Wang W, Zheng F. 2023. *CsTT8* regulates anthocyanin accumulation in blood orange through alternative splicing transcription. *Horticulture Research* 10:uhad190
48. Gao L, Wang W, Li H, Li H, Yang Y, et al. 2023. Anthocyanin accumulation in grape berry flesh is associated with an alternative splicing variant of VvMYBA1. *Plant Physiology and Biochemistry* 195:1–13
49. Qiu Z, Wang X, Gao J, Guo Y, Huang Z, et al. 2016. The tomato *Hoffman's anthocyaninless* gene encodes a bHLH transcription factor involved in anthocyanin biosynthesis that is developmentally regulated and induced by low temperatures. *PLoS One* 11:e0151067
50. Spelt C, Quattrocchio F, Mol J, Koes R. 2002. ANTHOCYANIN1 of *Petunia* controls pigment synthesis, vacuolar pH, and seed coat development by genetically distinct mechanisms. *The Plant Cell* 14:2121–35
51. Goff SA, Cone KC, Fromm ME. 1991. Identification of functional domains in the maize transcriptional activator C1: comparison of wild-type and dominant inhibitor proteins. *Genes & Development* 5:298–309
52. Kim S, Song H, Hur Y. 2021. Intron-retained radish (*Raphanus sativus* L.) *RsMYB1* transcripts found in colored-taproot lines enhance anthocyanin accumulation in transgenic *Arabidopsis* plants. *Plant Cell Reports* 40:1735–49
53. Jiang W, Liu T, Nan W, Jeewani DC, Niu Y, et al. 2018. Two transcription factors TaPpm1 and TaPpb1 co-regulate anthocyanin biosynthesis in purple pericarps of wheat. *Journal of Experimental Botany* 69(10):2555–67
54. Wang X, Chen X, Luo S, Ma W, Li N, et al. 2022. Discovery of a *DFR* gene that controls anthocyanin accumulation in the spiny *Solanum* group: roles of a natural promoter variant and alternative splicing. *The Plant Journal* 111:1096–109
55. Colanero S, Tagliani A, Perata P, Gonzali S. 2020. Alternative splicing in the *Anthocyanin fruit* gene encoding an R2R3 MYB transcription factor affects anthocyanin biosynthesis in tomato fruits. *Plant Communications* 1:100006
56. Chen D, Liu Y, Yin S, Qiu J, Jin Q, et al. 2020. Alternatively spliced *BnaPAP2.A7* isoforms play opposing roles in anthocyanin biosynthesis of *Brassica napus* L. *Frontiers in Plant Science* 11:983

Copyright: © 2024 by the author(s). Published by Maximum Academic Press, Fayetteville, GA. This article is an open access article distributed under Creative Commons Attribution License (CC BY 4.0), visit https://creativecommons.org/licenses/by/4.0/.